



SHRINKAGE IN REINFORCED CONCRETE STRUCTURES: A COMPUTATIONAL ASPECT

Viktor Gribniak¹, Gintaris Kaklauskas², Darius Bacinskas³

Dept of Bridges and Special Structures, Vilnius Gediminas Technical University,
Saulėtekio al. 11, LT-10223 Vilnius, Lithuania

E-mail: ¹Viktor.Gribniak@st.vgtu.lt, ²Gintaris.Kaklauskas@st.vgtu.lt, ³Darius.Bacinskas@st.vgtu.lt

Received 14 Dec. 2007; accepted 31 Jan. 2008

Abstract. This paper introduces the recent state of research on shrinkage of concrete. It reviews prediction models of shrinkage strain and curvature analysis methods of reinforced concrete members. New test data on concrete shrinkage has been presented. Various factors that influence shrinkage have been discussed. A calculation technique on short-term deformations of cracked reinforced concrete members including shrinkage has been introduced. The technique is based on *layer model* and smeared crack approach. Shrinkage influence on behaviour of reinforced concrete beams was investigated numerically and compared with test data reported in the literature. It has been shown that shrinkage has significantly reduced the cracking resistance and leads to larger deflections.

Keywords: shrinkage, reinforced concrete, cracking, short-term loading, creep.

1. Introduction

Mechanical loading, deleterious reactions, and environment loading can result in the development of tensile stresses in concrete structures. Furthermore, concrete shrink as it dries under ambient conditions. Tensile stresses occur when free shrinkage is restrained. The combination of high tensile stresses with low fracture resistance of concrete often results in cracking. This cracking reduces the durability of a concrete structure.

Effects of shrinkage and accompanying creep of concrete along with cracking provide the major concern to the structural designer because of the inaccuracies and unknowns that surround them. In general, these effects are taken into account of long-term deformation and prestress loss analysis of reinforced concrete (RC) structures. Though considered as long-term effects, shrinkage and creep also have influence on crack resistance and deformations of RC members subjected to short-term loading.

This paper introduces the recent state of research on shrinkage of concrete and reviews the prediction models. Factors that influence the behaviour of the shrunk reinforced concrete members are discussed. Shrinkage influence on short-term behaviour of reinforced concrete beams has been investigated numerically and compared with test data reported in the literature.

2. Factors, affecting shrinkage of concrete

Four main types of shrinkage associated with concrete are plastic shrinkage, autogenous shrinkage, carbonation shrinkage, and drying shrinkage. *Plastic shrinkage* is associated with moisture loss from freshly poured

concrete into the surrounding environment. *Autogenous shrinkage* is the early shrinkage of concrete caused by loss of water from capillary pores due to the hydration of cementitious materials, without loss of water into the surrounding environment. This type of shrinkage tends to increase at lower water to cementitious materials ratio and at a higher cement content of a concrete mixture. *Carbonation shrinkage* is caused by the chemical reactions of various cement hydration products with carbon dioxide present in the air. *Drying shrinkage* can be defined as the volumetric change due to the drying of hardened concrete. This type of shrinkage is caused by the diffusion of water from hardened concrete into the surrounding environment. Drying shrinkage is a volumetric change caused by the movement and the loss of water squeezing out from the capillary pores resulting in the development of tensile stresses, since the internal humidity attempts to make uniform with a lower environmental humidity. More recent investigation on various aspects of shrinkage is given in reference (Gribniak *et al.* 2007).

The magnitude of shrinkage deformations depends on concrete mixture proportions and material properties, method of curing, ambient temperature and humidity conditions, and geometry of the concrete element. In the analysis of concrete structures two components, i.e. drying and autogenous shrinkage, are taken into account. The ratio of autogenous and drying shrinkage in total shrinkage of concrete is schematically illustrated in Fig. 1 (Sakata & Shimomura 2004). In the case of normal-strength concrete, it is not a problem if shrinkage is treated without distinguishing between autogenous and drying shrinkage because for such concrete autogenous shrinkage strain varies between 20 and 110 micro-strains.

This is only 10 to 20 % of the long-term shrinkage (Siliman & Newton 2006). Consequently, autogenous shrinkage was neglected for many years. On the other hand, in the case of high-strength concrete (HSC), autogenous and drying shrinkage should be distinguished because the ratio of these shrinkages to total shrinkage varies with respect to age when concrete is exposed to drying conditions (Sakata & Shimomura 2004). The focus of shrinkage research today is to understand more the phenomenon of autogenous and drying shrinkage (Kovler & Zhutovskiy 2006).

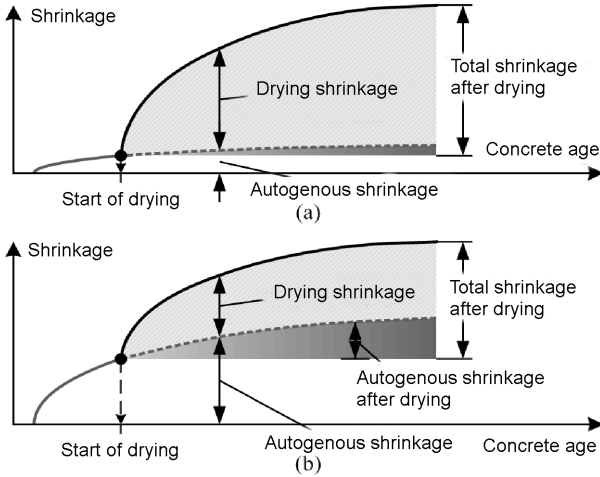


Fig. 1. Shrinkage strain components in normal (a) and high-strength (b) concrete (Sakata & Shimomura 2004)

3. Recent investigation on autogenous shrinkage modelling

Models reviewed in this chapter after deal with autogenous shrinkage, which is justly considered as the most important shrinkage components in HSC. Only the relevant aspects of researches are presented herein.

C. Hua, A. Erlacher and P. Acker (1995). Hua *et al.* presented a macroscopic scale analytical model of autogenous shrinkage (1995). It introduced a macroscopic stress induced by capillary depression and applied it to viscoelastic aging behaviour of the material.

Hardening cement paste is considered as a continuum medium with aging viscoelastic behaviour, which can be generally characterised by a creep function:

$$J(t, t') = \frac{1}{E(t')} + \varepsilon_{\infty}(t') \frac{[t - t']^{\alpha(t')}}{[t - t']^{\alpha(t')} + b(t')}, \quad (1)$$

where $\varepsilon_{\infty}(t')$, $\alpha(t')$, $b(t')$ are empirical parameters, which were obtained through a series of the experiments, as well as the values of Young's modulus. Shrinkage strain was calculated using the creep function:

$$\varepsilon(t) = \int_0^t J(t, t') [1 - 2\nu] d\Sigma^s(t'), \quad (2)$$

where $\Sigma^s(t')$ is macroscopic stress derived using the following equation:

$$\Sigma^s = P_c P = \left(-\frac{2\gamma}{r} \right) P, \quad (3)$$

where γ is surface tension of the liquid, r – radius of menisci curvature, P is total porosity of the material.

C. Hua, A. Erlacher and P. Acker (1997). The previous model represented autogenous deformations on the macroscopic scale, whereas the present model treats autogenous shrinkage at the scale of hydrating cement grains (Hua *et al.* 1997). In this model, the initial state is taken as the time of setting when continuous skeleton is formed and begins to undergo the capillary depression. To simplify the model, it was assumed that all cement grains are spherical and identical, and that distribution of grains is periodical. This allows working on periodic cell.

In the mechanical model the material is composed of three constituents with locally non-ageing properties. *Anhydrous cement* was considered as elastic isotropic, characterised by *Young's* modulus and *Poisson's* ratio, and modelled by internal hydrate layers. *Hydrates* and *immobilised water* was considered as a viscoelastic isotropic component. The viscoelastic deformation of each layer begins when it forms. Accordingly, each new layer is deposited on layers already deformed by capillary depression and thus each hydrate layer has its own history of deformation. This model allows modelling a macroscopically ageing material, while constituents have a very simple behaviour.

E. A. B. Koenders and K. van Breugel (1997). This model uses thermodynamic approach to determine autogenous shrinkage of hardening cement paste (Koenders & van Breugel 1997). In this model, variation in surface tension is considered as the major driving force of autogenous shrinkage. Assuming a cylindrical pore shape, pore size distribution model was initially established, which is described mathematically by the function:

$$V_p(d) = a \ln(d/d_0), \quad (4)$$

where $V_p(d)$ is volume of all capillary pores with diameter $\leq d$; d_0 is the minimum capillary pore diameter was set to $0,002 \mu\text{m}$, and a is the constant which reflects the increase of pore space with respect to the pore diameter.

Autogenous deformations are calculated using *Bangham* formula (Bangham & Fackhoury 1931):

$$\Delta l/l = \lambda \cdot \Delta\gamma. \quad (5)$$

The proportionality factor λ utilises the empty pore wall area found from pore size distribution and is calculated according to the equation

$$\lambda = \frac{\Sigma \cdot \rho}{3E}, \quad (6)$$

where Σ is pore wall area of empty pores, ρ – specific mass and E – elasticity modulus of the material.

Ishida *et al.* (1998). This model was derived from micro-mechanical physics of water in pore structure of concrete (Ishida *et al.* 1999). The capillary tension was assumed to be the driving force of autogenous and drying shrinkage.

The material properties of ageing concrete were obtained by the analysis considering the interrelation of hydration, moisture transport and pore structure development process. Cement hydration model provided hydration level of each mineral and temperature development due to heat of hydration. The capillary tension is assumed a driving force of both autogenous and drying shrinkage. This method allows modelling a macroscopically ageing material with viscoelastic behaviour, and additionally taking into account a loading history.

4. Shrinkage and creep prediction techniques

Designers typically use one of two code methods to estimate creep and shrinkage strain in concrete, ie either *Eurocode 2* or *ACI 318*. *Eurocode 2* is based on the *CEB-FIP MC 90* model recommended by the *Euro-International Committee*, and *ACI 318* is based on the *ACI 209* model recommended by the *American Concrete Institute* (Meyerson *et al.* 2002: 8). This chapter presents three shrinkage and creep predictions models, namely the *CEB-FIP MC 90* model, *ACI 209* model, and *Bazant & Baweia (B3)* model.

4.1. Modulus of elasticity

The modulus of elasticity is an input parameter to the creep compliance. It is defined as the tangent modulus of elasticity at the origin of the stress-strain diagram and can be estimated from the mean compressive cylinder strength and the concrete age. The tangent modulus E_c is approximately equal to the secant modulus E_{cm} of unloading which is usually measured in tests. Formulas according to some relevant design codes are shown in Table 1, where f_{cm} is the mean concrete cylinder compressive strength at the age of 28 days [MPa].

Table 1. Formulas for the modulus of elasticity at age of 28 days

Design code	Formula for E_c [MPa]
<i>Eurocode 2</i>	$E_{cm} = 22000(0,1 \cdot f_{cm})^{0,3}$
<i>CEB-FIP Model Code 1990</i>	$E_{cm} = 9980\sqrt[3]{f_{cm}}$
<i>ACI 318</i>	$E_c = 4733\sqrt{f_{cm}}$

Besides the concrete strength, the elastic modulus depends also on the type of the aggregate, the curing conditions and the test method. The influences of these factors are largely responsible for the significant scatter which can be observed when experimental values of the modulus of elasticity are plotted against the concrete strength (Takács 2002: 14). Test result of the elastic modulus is usually available for major structures but it is very rare that at least a short-term creep test is carried out (Takács 2002: 30). Applying the measured elastic modulus into creep analysis may improve the deformation prediction or may corrupt it. A short-term creep test is therefore a recommended option for major structures. Under precise and careful implementation a creep test with a load duration as short as two days can be adequate

to adjust the theoretical creep compliance with appreciable accuracy (Bazant *et al.* 1999).

4.2. CEB-FIP Model Code 1990 (MC 90)

The equations presented here were published in the final draft of the *MC 90* (CEB 1991). The model is valid for normal density concrete with grade up to C80 and exposed to a mean relative humidity in the range of 40 to 100 %. At the time when the code was prepared very limited information on concrete with a characteristic strength higher than 50 MPa were available and therefore the models should be used with caution in that strength range.

Creep. The relationship between the total stress-dependent strain and the stress is described with the compliance function which is written as

$$J(t, t_0) = \frac{1}{E_c(t_0)} + \frac{\Phi(t, t_0)}{E_c}, \quad (7)$$

where $\Phi(t, t_0)$ is the creep coefficient; t_0 – the age of concrete at loading [days]; $E_c = 1,1 \cdot E_{cm}$ – the tangent modulus at the age of 28 days [MPa]; $E_c(t_0)$ – the tangent modulus at the age of loading t_0 [MPa].

The creep coefficient is estimated from

$$\Phi(t, t_0) = \Phi_0 \beta_c(t - t_0), \quad (8)$$

where Φ_0 is the notional creep coefficient; $\beta_c(t - t_0)$ – the time function to describe the development of creep with time. The notional creep coefficient is derived from

$$\Phi_0 = \Phi_{RH} \beta(f_{cm}) \beta(t_0) \quad (9)$$

$$\Phi_{RH} = 1 + \frac{1 - RH/100}{0,1\sqrt[3]{h_0}}; \quad \beta(f_{cm}) = \frac{16,8}{\sqrt{f_{cm}}}$$

$$\beta(t_0) = \frac{1}{0,1 + t_0^{0,2}}; \quad h_0 = \frac{2A_c}{u},$$

where RH is the relative humidity of the ambient environment [%]; h_0 – the notional size of the structural member [mm]; A_c – the area of the cross-section of the structural member [mm²]; u – the perimeter of the cross-section in contact with the atmosphere [mm].

The time development function for the creep coefficient is written as

$$\beta_c(t - t_0) = \left(\frac{t - t_0}{\beta_H + t - t_0} \right)^{0,3} \quad (10)$$

$$\beta_H = 1,5 \left[1 + (0,012 \cdot RH)^{18} \right] h_0 + 250 \leq 1500.$$

Shrinkage. The shrinkage strain is calculated as

$$\varepsilon_{cs}(t, t_s) = \varepsilon_{cs0} \beta_s(t - t_s), \quad (11)$$

where ε_{cs0} is the notional shrinkage coefficient; β_s – the time function to describe the development of shrinkage with time; t_s – the age of concrete when drying begins [days]. The notional shrinkage coefficient can be estimated from

$$\varepsilon_{cs0} = \varepsilon_s(f_{cm}) \beta_{RH}, \quad (12)$$

where

$$\varepsilon_s(f_{cm}) = [160 + 10\beta_{sc}(9 - 0,1f_{cm})] \cdot 10^{-6}$$

$$\beta_{RH} = \begin{cases} -1,55 \cdot \left[1 - \left(\frac{RH}{100}\right)^3\right], & RH < \beta_{s1} \cdot 99 \% \\ 0,25, & RH \geq \beta_{s1} \cdot 99 \% \end{cases} \quad (13)$$

where β_{sc} is a coefficient which depends on the cement type, 4 for slowly hardening cement, 5 for normal and rapid hardening cement and 8 for rapid hardening high strength cement; factor β_{s1} was assumed equal to 1,0. RH in Eq (13) should be not less than 40 %.

The development of shrinkage with time is given by

$$\beta_s(t-t_s) = \sqrt{\frac{t-t_s}{0,035 \cdot h_0^2 + t-t_s}}. \quad (14)$$

The influence of mean temperature other than 20° C can be also taken into account. With the decreasing temperature both the notional creep coefficient and the notional shrinkage coefficient are decreasing and their development with time are decelerated.

4.3. The 1999 update of the CEB-FIP MC 1990

The models were published in the *fib Bulletin (FIB 1999)*. The primary intention with the update was to improve the prediction models for high-strength concrete and further extend the validity of the models to high-performance concrete.

Creep. The updated creep model was in fact first published in *Eurocode 2 (CEN 2001)*. It is closely related to the model in the *MC 90 (CEB 1991)*, but three strength dependent coefficients were introduced into the original model. The extended model is valid for both normal strength concrete and high performance concrete up to concrete cylinder strength of 110 MPa. Three coefficients were introduced into the *MC 90* model:

$$\alpha_1 = \left(\frac{35}{f_{cm}}\right)^{0,7}; \quad \alpha_2 = \left(\frac{35}{f_{cm}}\right)^{0,2}; \quad \alpha_3 = \left(\frac{35}{f_{cm}}\right)^{0,5}. \quad (15)$$

Coefficients α_1 and α_2 are meant to adjust the notional creep coefficient through the Φ_{RH} term. Coefficient α_3 is meant to be the adjustment for the time dependency function. Eqs (9) and (10) have been rearranged in following form:

$$\Phi_{RH} = \alpha_2 \left(1 + \alpha_1 \frac{1 - RH/100}{0,1\sqrt[3]{h}}\right); \quad (16)$$

$$\beta_H = 1,5 \left[1 + (0,012RH)^{18}\right] h_0 + 250\alpha_3 \leq 1500\alpha_3.$$

Shrinkage. The shrinkage model represents a major change. The total shrinkage is subdivided into the autogenous shrinkage component and the drying shrinkage component. With this approach it was possible to formulate a model which is valid for both normal strength concrete and high performance concrete having compressive strength up to 120 MPa.

The total shrinkage strain at time t is calculated as

$$\varepsilon_{cs}(t, t_s) = \varepsilon_{cas}(t) + \varepsilon_{cds}(t, t_s) \quad (17)$$

with

$$\varepsilon_{cas}(t) = \varepsilon_{cas0}(f_{cm}) \cdot \beta_{as}(t)$$

$$\varepsilon_{cds}(t, t_s) = \varepsilon_{cds0}(f_{cm}) \cdot \beta_{RH}(RH) \cdot \beta_{ds}(t-t_s), \quad (18)$$

where $\varepsilon_{cas}(t)$ and $\varepsilon_{cds}(t, t_s)$ are the autogenous and drying shrinkage strain at time t , respectively; $\varepsilon_{cas0}(f_{cm})$ and $\varepsilon_{cds0}(f_{cm})$ are the notional autogenous and drying shrinkage coefficients, respectively; $\beta_{as}(t)$ and $\beta_{ds}(t-t_s)$ are the time development function for autogenous and drying shrinkage, respectively; $\beta_{RH}(RH)$ is the coefficient taking into account the effect of relative humidity on drying; t – the concrete age [days]; t_s – the age of concrete, when drying begins [days]; $t-t_s$ – the duration of drying [days].

The formulations for estimating the autogenous shrinkage are written as

$$\varepsilon_{cas0}(f_{cm}) = -\alpha_{as} \left(\frac{0,1 \cdot f_{cm}}{6 + 0,1 \cdot f_{cm}}\right)^{2,5} \cdot 10^{-6} \quad (19)$$

$$\beta_{as}(t) = 1 - e^{-0,2\sqrt{t}},$$

where α_{as} is a coefficient which depends on the cement type, 800 for slowly hardening cement, 700 for normal and rapidly hardening cement and 600 for rapidly hardening high-strength cement.

In *Eurocode 2 (CEN 2001)* autogenous shrinkage is calculated using the following equation:

$$\varepsilon_{cas0}(f_{ck}) = -2,5(f_{ck} - 10) \cdot 10^{-6}. \quad (20)$$

The formulations for estimating the drying shrinkage are written as

$$\varepsilon_{cds0}(f_{cm}) = \left[(220 + 110\alpha_{ds1}) e^{-0,1\alpha_{ds2}f_{cm}} \right] \cdot 10^{-6}$$

$$\beta_{s1} = (35/f_{cm})^{0,1}, \quad (21)$$

where α_{ds1} is a coefficient which depends on the cement type, 3 for slowly hardening cement, 4 for normal and rapidly hardening cement and 6 for rapidly hardening high-strength cement; α_{ds2} is a coefficient which depends on the cement type, 0,13 for slowly hardening cement, 0,11 for normal and rapidly hardening cement and 0,12 for rapidly hardening high-strength cement. Coefficients β_{RH} and $\beta_s(t-t_s)$ are derived according to formulas (13) and (14) using factor β_{s1} calculated by Eq (21). The effect of ageing on the elastic modulus can be taken into account using the following equation:

$$E_c(t) = \beta_E(t) E_c, \quad (22)$$

where $E_c(t)$ is the modulus of elasticity of the concrete at age of t days [MPa], $\beta_E(t)$ – the time development function for the elastic modulus. This function can be derived from the relationship

$$\beta_E(t) = \left(\exp \left\{ s \left[1 - \sqrt{\frac{28}{t}} \right] \right\} \right)^\alpha, \quad (23)$$

where t is the concrete age [day]; s – a coefficient which depends on the cement type, 0,20 for rapid hardening high-strength cement, 0,25 for normal and rapid hardening cement and 0,38 for slowly hardening cement; α is parameter assumed equal to 0,3.

4.4. ACI 209 model

ACI 209 model (ACI Committee 209 1998) recommended by the American Concrete Institute to estimate shrinkage and creep strain.

Creep. This model uses a hyperbolic function to represent the creep-time relationship:

$$\Phi(t, t_0) = \frac{(t - t_0)^{0,6}}{10 + (t - t_0)^{0,6}} \Phi(t_0), \quad (24)$$

where t_0 – the age of the concrete at first loading [days]; $t - t_0$ – the duration of loading [days]; $\Phi(t_0)$ – the final creep coefficient and expressed as

$$\Phi(t_0) = 2,35 \prod_{i=1}^6 \gamma_{c,i}, \quad (25)$$

where $\gamma_{c,i}$, $i = 1 \dots 6$ are empirical coefficients with account for parameters affecting the creep magnitude.

Coefficient $\gamma_{c,1}$ accounts the concrete age at the time of the first loading, t_0 .

$$\gamma_{c,1} = \begin{cases} 1,25 \cdot t_0^{-0,118}, & t_0 > 7 \text{ days; moist cured,} \\ 1,13 \cdot t_0^{-0,094}, & t_0 > 1-3 \text{ days; steam cured.} \end{cases} \quad (26)$$

Coefficient $\gamma_{c,2}$ includes the effect of variations in the ambient relative humidity, RH [%]:

$$\gamma_{c,2} = 1,27 - 0,0067 \cdot RH, \quad RH > 40 \%. \quad (27)$$

Coefficient $\gamma_{c,3}$ accounts the size and shape of the member. Two alternative methods are given for the estimation of $\gamma_{c,3}$ (ACI Committee 209 1998). Here presented technique is based on the average thickness $h_{0,ACI} = 2h_0$ [see Eq (9)] and recommended for average thicknesses up to about 305 to 380 mm. For average thickness of the member less than 150 mm, $\gamma_{c,3}$ is obtained from Table 2.

For average thickness of members greater than 150 mm and up to 380 mm, $\gamma_{c,3}$ is calculated by the equation

$$\gamma_{c,3} = \begin{cases} 1,14 - 0,00092 \cdot h_{0,ACI}; & t - t_0 \leq 1 \text{ year,} \\ 1,10 - 0,00067 \cdot h_{0,ACI}; & t - t_0 > 1 \text{ year.} \end{cases} \quad (28)$$

Table 2. Correction factor accounts size and shape of the member for deriving creep and shrinkage

Effects	Average thickness $h_{0,ACI}$				
	51	76	104	127	152
Creep	1,30	1,17	1,11	1,04	1,00
Shrinkage	1,35	1,25	1,17	1,08	1,00

Coefficients $\gamma_{c,4} \dots \gamma_{c,6}$ depend on the composition of the concrete

$$\begin{aligned} \gamma_{c,4} &= 0,82 + 0,00264 \cdot s; \quad s > 130 \text{ mm;} \\ \gamma_{c,5} &= 0,88 + 0,0024 \cdot \psi; \quad \psi < 40 \text{ or } \psi > 60 \%; \\ \gamma_{c,6} &= 0,46 + 0,09 \cdot \alpha < 1,0; \quad \alpha > 8 \%, \end{aligned} \quad (29)$$

where s is the slump of the fresh concrete [mm]; ψ – the ratio of the fine aggregate to total aggregate by weight [%] and α is the air content [%]. These coefficients in undefined intervals are assumed equal to 1,0.

Under a constant stress σ_0 first applied at age t_0 , the load-dependent strain at time t is derived from the relationship:

$$\varepsilon(t) = \frac{\sigma_0}{E_c(t_0)} [1 + \Phi(t, t_0)], \quad (30)$$

where $E_c(t_0)$ is obtained from the equation presented in Table 1. The concrete strength at age t_0 may be obtained from the 28 day strength by the equation

$$f_c(t) = \frac{t_0}{\alpha + \beta \cdot t_0} f_c(28), \quad (31)$$

where α and β depend on the cement type and curing conditions. For normal Type I cement, these coefficients are assumed equal to 4 and 0,85 (for moist curing) and 1 and 0,95 (for steam curing), respectively.

Shrinkage. The shrinkage strain at time t measured from the start of drying is calculated by following equation:

$$\varepsilon_{cs}(t) = \begin{cases} \varepsilon_{cs,u} t / (35 + t); & \text{moist cured,} \\ \varepsilon_{cs,u} t / (55 + t); & \text{steam cured,} \end{cases} \quad (32)$$

where $\varepsilon_{cs,u}$ is the ultimate shrinkage at time infinity and represents the product of the applicable correction factors:

$$\varepsilon_{cs,u} = 780 \times 10^{-6} \prod_{i=1}^7 \gamma_{cs,i}, \quad (33)$$

where $\gamma_{cs,i}$, $i = 1 \dots 7$ are empirical coefficients with account for parameters affecting the shrinkage magnitude.

Coefficient $\gamma_{cs,1}$ includes the effect of variations in the ambient relative humidity, RH [%]:

$$\gamma_{cs,1} = \begin{cases} 1,40 - 0,0102 \cdot RH, & 40 \leq RH \leq 80 \%, \\ 3,00 - 0,030 \cdot RH, & 80 < RH \leq 100 \%. \end{cases} \quad (34)$$

Coefficient $\gamma_{cs,2}$ accounts for the size and shape of the member. Two alternative methods as in creep analysis are given in (ACI Committee 209 1998) for estimating the $\gamma_{cs,2}$. Herein presented technique is based on the average thickness $h_{0,ACI}$ (Table 2). For average thickness of members greater than 150 mm and up to 380 mm, $\gamma_{cs,2}$ is calculated using the equation

$$\gamma_{cs,2} = \begin{cases} 1,23 - 0,0015 \cdot h_{0,ACI}; & t - t_0 \leq 1 \text{ year,} \\ 1,17 - 0,0011 \cdot h_{0,ACI}; & t - t_0 > 1 \text{ year.} \end{cases} \quad (35)$$

Coefficients $\gamma_{cs,3} \dots \gamma_{cs,7}$ depend on the composition of the concrete

$$\begin{aligned} \gamma_{cs,3} &= 0,89 + 0,00161 \cdot s; \quad s > 130 \text{ mm}; \\ \gamma_{cs,4} &= \begin{cases} 0,30 + 0,014 \cdot \psi; & \psi \leq 50 \% \\ 0,90 + 0,002 \cdot \psi; & \psi > 50 \% \end{cases} \\ \gamma_{cs,5} &= 0,95 + 0,008 \cdot \alpha; \quad \alpha > 8 \% \\ \gamma_{cs,6} &= 0,75 + 0,00061 \cdot c, \end{aligned} \quad (36)$$

where c is cement content in concrete [kg/m^3]; other parameters are analogous to Eq (29). These coefficients in undefined intervals are assumed equal to 1,0.

Table 3. Shrinkage correction factor accounts for initial moist curing period

Curing period, days	1	3	7	14	28	90
$\gamma_{cs,7}$	1,2	1,1	1,0	0,93	0,86	0,75

Coefficient $\gamma_{cs,7}$ accounts for variations in the period of initial moist curing and is presented in Table 3. For a concrete which is steam cured for a period of between one and three days $\gamma_{cs,7} = 1,0$.

4.5. Bažant & Baweia (B3) model

The complete description of the B3 model can be found in (Bažant & Baweja 1995a, 1995b).

Creep. An important feature of the B3 creep model is that the compliance function is decomposed into the instantaneous response, the compliance function for basic creep and the additional compliance function for drying creep. The creep compliance is written as

$$J(t, t_0) = \frac{1}{E_0} + C_0(t, t_0) + C_d(t, t_0, t_s), \quad (37)$$

where E_0 is the so-called asymptotic modulus; $C_0(t, t_0)$ and $C_d(t, t_0, t_s)$ are the compliance function for basic and drying creep, respectively.

The instantaneous response is defined with the so-called asymptotic modulus, E_0 , which is not the same as the conventional static modulus. The asymptotic modulus is considered age independent. Its value is higher than the real elastic modulus and it can be estimated as $E_0 \approx 1,5E$. According to Bažant, it is more convenient to use the asymptotic modulus because concrete exhibits a pronounced creep even after a short loading.

Shrinkage. The shrinkage strain at time t is defined as:

$$\varepsilon_{cs}(t, t_0) = -\varepsilon_{cs\infty} k_{RH} S(t), \quad (38)$$

where

$$\begin{aligned} \varepsilon_{cs\infty} &= \alpha_1 \alpha_2 \left(1,9 \times 10^{-2} w^{2,1} f_{cm}^{-0,28} + 270 \right) \times 10^{-6}, \\ S(t) &= \tanh \sqrt{(t - t_0) / \tau_{sh}}, \end{aligned} \quad (39)$$

where $\varepsilon_{cs\infty}$ is the ultimate shrinkage; $S(t)$ – the time function for shrinkage; α_1 and α_2 are the correlation terms for effects of cement type and curing conditions,

respectively; w – the water content; k_{RH} – humidity dependence factor; t – the age of concrete; t_0 – the age, when during begins; τ_{sh} – the size dependence factor.

The B3 model takes into account the influence of the material composition directly. Besides model parameters, which are considered in previously reviewed models, the cement content, the water-cement ratio, the aggregate-cement ratio and the water content are taken into account.

5. Experimental investigations of concrete shrinkage

An important but often overlooked property of creep and shrinkage prediction models is the expected error of the prediction. Creep and shrinkage are among the most uncertain mechanical properties of concrete. The theoretical models only predict the mean tendencies based on observations in available experimental data. In any particular prediction the effect of a certain parameter may be overestimated or underestimated (Takács 2002: 17). This chapter introduces experimental shrinkage measurements performed by the authors and performs a comparison with the predictions by Eurocode 2 and ACI 209 predictions against these data.

Table 4. Mix proportion of the experimental specimens

Explanation	Measure	Amount
Sand, 0/4 mm	kg/m^3	$905 \pm 2 \%$
Crushed aggregate, 5/8 mm	kg/m^3	$388 \pm 1 \%$
Crushed aggregate, 11/16 mm	kg/m^3	$548 \pm 1 \%$
Cement CEM I 42,5 N	kg/m^3	$400 \pm 0,5 \%$
Water	kg/m^3	$123,8 \pm 5 \%$
Concrete plasticiser <i>Muraplast</i>	kg/m^3	$2 \pm 2 \%$

The tests were performed in the laboratory of Vilnius Gediminas Technical University in 2005. The experimental specimens were cured under the laboratory conditions at average relative humidity (RH) 64,7 % and average temperature 13,1 °C. Concrete mix proportion is given in Table 4. The ordinary Portland cement and crushed aggregate (16 mm maximum nominal size) were used. Water/cement and aggregate/cement ratio by weight were taken as 0,42 and 2,97, respectively.

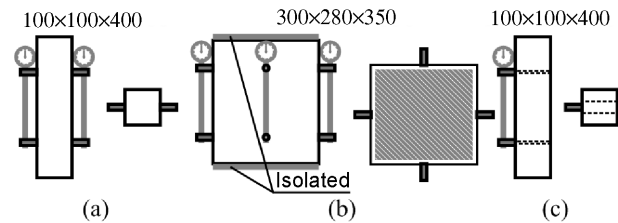


Fig. 2. Specimens for measuring the shrinkage deformations

Free shrinkage measurements were performed on prisms of $100 \times 100 \times 400$ mm and $280 \times 300 \times 350$ mm in size. The specimens and instrumentation for measuring the shrinkage deformations are shown in Fig. 2. Steel gauge studs, with the base 200 mm, were either glued on the concrete surface (Figs 2a and 2b) or embedded in fresh

concrete (Fig. 2c). In the latter case, free shrinkage measurements were initiated in 24 h after casting, whereas measurements on other prisms were started in 3-4 days.

Shrinkage deformation variation in time is shown in Fig. 3(a). It is clearly seen the difference between the deformations measured in 280 × 300 × 350 mm and 100 × 100 × 400 mm prisms. The latter effect is caused by the only factor, i.e. the difference in the cross-section.

The size conversion factors obtained from the tests and predicted by the Eurocode 2 (EC 2) and ACI 209 design code formulas are given in Table 5. It is seen that the EC 2 predictions were adequate, whereas the ACI technique has significantly overestimated the factor. Fig. 3b plots experimental points obtained for both types of specimens using the experimentally derived size correction factor (Table 5). The predicted shrinkage variation curves using the EC 2 and ACI 209 methods for 280 × 300 × 350 mm prisms, based on averaged parameters of test specimens are also shown in Fig. 3b.

It can be stated that the averaged curve obtained from the test results falls in between the code curves. Numerical results in Table 6 support the graphical data.

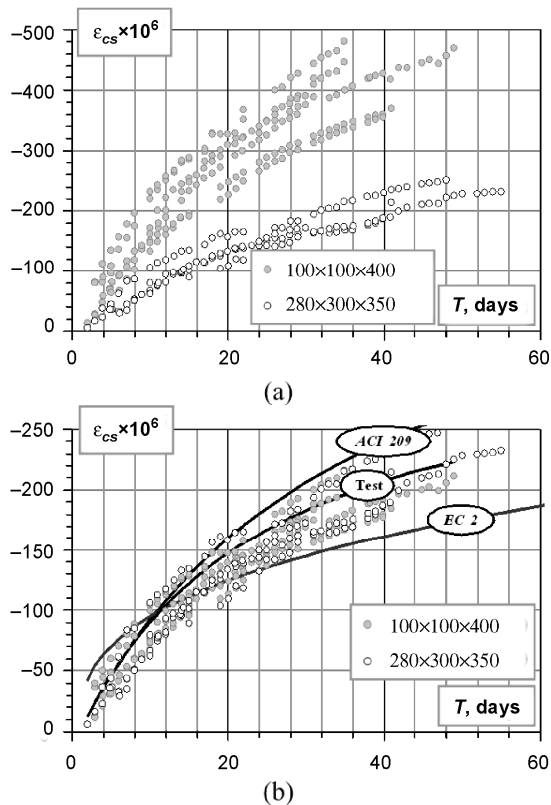


Fig. 3. Free shrinkage deformations: measured in different size prisms (a) and reduced to size of test beams (b)

Table 5. Size factor (converting shrinkage strain from 100 × 100 × 400 mm prisms to 280 × 300 × 350 mm prisms)

Beams	EC 2	ACI 209	Experimentally derived
S-1, S-1R	0,494	0,678	0,45
S-2, S-2R	0,495		0,45
S-3, S-3R	0,498		0,50
S-4, S-4R	0,520		0,45

Table 6. Shrinkage deformations of 280 × 300 × 350 mm prisms at test day ($\epsilon_{cs} \times 10^6$)

Beam	t_0	Predicted by		Experimentally measured
		EC 2	ACI 209	
S-1	4 days	-165,6	-253,5	-194,6
S-1R	4 days	-164,1	-250,6	-188,2
S-2	3 days	-141,6	-192,2	-152,6
S-2R	3 days	-143,3	-196,2	-155,7
S-3	4 days	-132,0	-191,1	-137,0
S-3R	4 days	-133,3	-194,6	-139,6
S-4	4 days	-152,5	-203,3	-172,0
S-4R	4 days	-154,5	-209,0	-177,0

6. Creep and shrinkage models in comparison

Experimental results of creep and shrinkage are marked with a large scatter, at least from the perspective of existing approach in modelling. The creep compliance and the shrinkage strain given by the theoretical models are seen as the expected average value of the responses and the prediction is also characterised by the corresponding measure of variation. Consequently, the structural response should be considered as a statistical variable rather than a deterministic value. The expected statistical variation has to be taken into account in the structural design. The reported coefficient of variation is 20 % for the creep compliance and 35 % for the shrinkage strain for the MC 90 (CEB 1991). The same values are 23 % and 34 % for the B3 model (Bazant & Baweja 1995a, 1995b).

A recent comparison of models discussed in Chapter 4 using the distribution of residuals of the creep predictions showed that the Eurocode 2, ACI 209 and B3 models overestimated the creep for 39 %, 23 % and 42 %, of the total number of data points and underestimated the creep for 61 %, 77 % and 58 %, respectively (Al-Manaseer & Lakshmikantham 1999). The mean coefficient of variation for the residuals for the Eurocode 2, ACI 209 and B3 models were 31 %, 38,6 % and 32 %, respectively. The prediction model parameters and corresponding limitations are presented in Table 7. In this table A/C is aggregate-to-cement ratio; W/C is water-to-cement ratio; t_0 or t_s are the age of concrete at loading and beginning of a shrinkage, respectively.

A comprehensive investigation into accuracy of shrinkage and creep prediction models was performed by Meyerson *et al.* (2002: 46). It has been shown that the Eurocode 2 predicts the creep and shrinkage strain of concrete with the best precision and accuracy. Al-Manaseer & Lam (2005) performed a comparative analysis of shrinkage and creep models using experimental data from RILEM Data Bank. It has been found that B3 is the best model to predict shrinkage and creep effects; Eurocode 2 predictions of creep were also considered accurate.

Schellenberg *et al.* (2005) compared the creep and shrinkage predictions made by Eurocode 2 and ACI 209. It has been stated that the differences between codes can be significant in early stages of construction. For longer periods of time there was found no essential difference between predictions. It has been pointed out that the most

important thing is taking the shrinkage and creep effects into consideration, while it is only of a secondary importance which code is applied.

Table 7. Models variables and limitations

Variable	EC 2	ACI 209	B3
f_{cm} [MPa]	20–120	–	17–69
A/C	–	–	2,5–13,5
Cement [kg/m ³]	–	–	160–720
W/C	–	–	0,35–0,85
RH [%]	40–100	40–100	40–100
Cement type	I, II or III	I or III	I, II or III
t_0 or t_s (moist cured)	–	≥ 7 days	$t_s \leq t_0$
t_0 or t_s (steam cured)	–	$\geq 1-3$ days	$t_s \leq t_0$

7. Influence of shrinkage and creep on deformations of RC structures

Under restraining conditions, shrinkage is always associated with creep which relieves the stresses induced by shrinkage. In general, shrinkage and creep are taken into account of long-term deformation and prestress loss analysis of concrete structures (Zamblauskaitė et al. 2005). Though considered as a long-term effect, shrinkage may significantly reduce crack resistance and increase deformations of RC members subjected to short-term loading (Bischoff 2001; Sato et al. 2007). However, most of the known techniques do not include these effects in a short-term analysis.

To better understand how volumetric changes of hardened concrete can result in cracking, Fig. 4(a) compares the time dependent strength (cracking resistance) development with the time dependent residual stresses that develop. If strength and residual stress development are plotted as shown in Fig. 4(a), it is likely that the specimen will crack when these two lines intersect. Similarly, it follows that if strength of the concrete is always greater than the developed stresses, no cracking will occur.

The residual stress that develops in concrete as a result of restraint may sometimes be difficult to quantify. This residual stress cannot be computed directly by multiplying the free shrinkage strain by the elastic modulus (ie Hooke’s Law) since stress relaxation occurs. Stress relaxation is similar to creep. However, while creep can be thought of as the time dependent deformation due to a sustained load, stress relaxation is a term used to describe the reduction in stress under a constant deformation. This reduction is illustrated in Fig. 4b in which a specimen of original length (I) is exposed to drying and a uniform shrinkage strain uniformly developed across the section. If the specimen is unrestrained, the applied shrinkage would cause the specimen to undergo a change in length of ΔL^+ (II). To maintain the condition of perfect restraint (ie no length change) a fictitious load can be envisioned to be applied (III). However, it should be noted that, if the specimen was free to displace under this fictitious loading, the length of the specimen would increase (due to creep) by an amount ΔL^- (IV). Again, to maintain a perfect restraint (ie no length change) an opposing fictitious stress is applied (V) resulting in an overall reduction in

shrinkage stress (VI). This illustrates that creep can play a very significant role in determining the magnitude of stresses that develop at early ages and has been estimated to relax the stresses by 30 % to 70 % (Weiss 1999: 145).

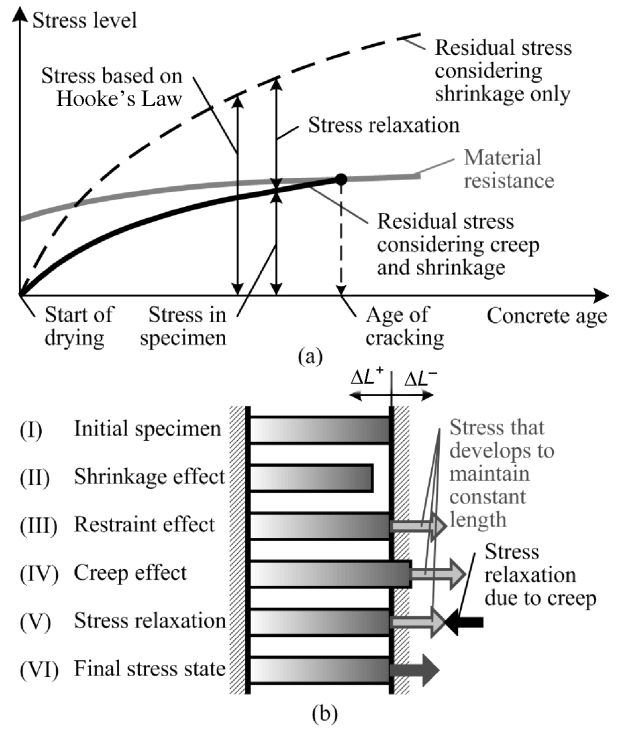


Fig. 4. Stresses in a restrained concrete member due to shrinkage and accompanying creep (Weiss 1999: 145): a – stress development and b – conceptual description of relaxation

Deformational behaviour of plain and RC members due to shrinkage has been analysed under the assumption of uniform distribution of shrinkage strain across the section. As shown in Figs 5a and 5c, shrinkage of an isolated plain concrete member would merely shorten it without causing camber. Reinforcement embedded in a concrete member provides restraint to shrinkage leading to compressive stresses in reinforcement and tensile stresses in concrete (Figs 5b, 5d). If the reinforcement is not symmetrically placed in a section, shrinkage causes non-uniform stress and strain distribution within the height of the section (Fig. 6). The maximal tensile stresses appear in the extreme concrete fibre, close to a larger concentration of reinforcement.

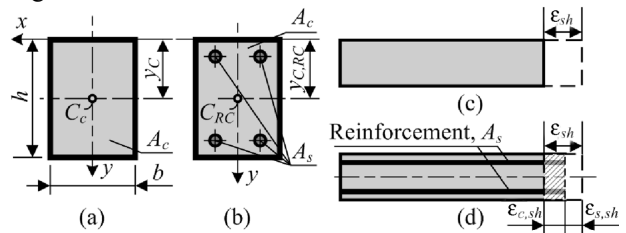


Fig. 5. Deformations of concrete and RC member due to shrinkage (Gribniak et al. 2007): a – plain concrete member; b – symmetrically reinforced section; c – free shrinkage deformation; d – deformations in a symmetrically reinforced element due to restrained shrinkage

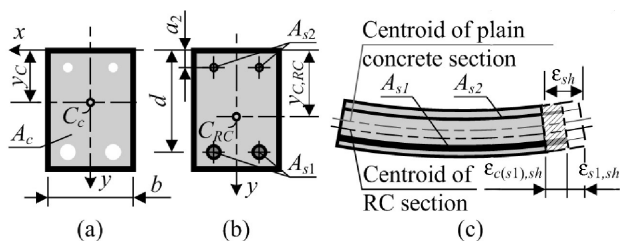


Fig. 6. Deformations of asymmetrically RC member due to shrinkage (Gribniak *et al.* 2007): a – plain concrete net section; b – asymmetrically reinforced section; c – deformations in asymmetrically reinforced element due to restrained shrinkage

8. Prediction methods for shrinkage deflection

It is common for all approximate methods based on beam model to calculate the mid-deflection f by the formula representing an approximate integration of curvature of cracked cross-sections:

$$f = s \cdot \kappa \cdot l^2. \tag{40}$$

In the above, s is the factor depending on a loading case covering the shape of moment distribution; κ – the curvature; l – the beam span. The crucial point is how to estimate the shrinkage curvature. This chapter presents some methods for predicting this curvature.

8.1. Eurocode 2 method

It is pointed out in *Eurocode 2* (CEN 2001) that time dependent deformations of concrete from creep and shrinkage shall be taken into account. Shrinkage curvature κ_{cs} may be assessed using the following expression:

$$\kappa_{cs} = \varepsilon_{cs} \alpha_e \frac{S}{I}; \quad \alpha_e = \frac{E_s}{E_{c,eff}}; \quad E_{c,eff} = \frac{E_{cm}}{1 + \Phi}, \tag{41}$$

where ε_{cs} is the free shrinkage strain (see Eq (17)); S – the first moment of area of the reinforcement about the centroid of the section; I – the second moment of area of the section; Φ – the creep coefficient relevant for the load and time interval (see Eq (8)).

8.2. ACI 435 method

Based on the ACI 435 (ACI Committee 435 2003), a long-term curvature at time t is the sum of three components corresponding to the influence of external loading, creep and shrinkage. Shrinkage curvature is determined, using the *equivalent tensile force* method, by the following formula:

$$\kappa_{cs} = \varepsilon_{cs} \frac{A_c e_c}{I_{eff}}; \quad E_{c,eff} = \frac{E_c}{1 + \chi \Phi}, \tag{42}$$

where ε_{cs} is the shrinkage strain (see Eq (32)); e_c is the distance between the centroid of plain concrete area A_c and the centroid of the age-adjusted transformed section (Fig. 6); I_{eff} – moment of inertia about the centroid of the age-adjusted transformed section composed of A_c plus $\bar{n} = E_s/E_{c,eff}$ multiplied by areas of reinforcements; χ – the ageing coefficient (can be assumed 1,0); Φ – the creep coefficient (see (24)).

8.3. Modified equivalent tensile force method

The *equivalent tensile force* method (a fictitious elastic analysis) has been used in various forms at least since 1936, for instance see (Branson 1977: 168). This method was modified in (ACI Committee 435 2003) using $0,5E_c$ and the gross section properties for better results, is given by next equation:

$$\kappa_{cs} = 2 \frac{N_{cs} e_g}{E_{c,eff} I_g}; \quad N_{cs} = \varepsilon_{cs} E_s (A_{s1} + A_{s2}), \tag{43}$$

where e_g is the distance between the centroid of the plain concrete section and the extreme tensile fibre (Fig. 6); I_g refers to plain concrete section, other notations are the same as in Eq (41).

8.4. Miller’s method

Miller’s method (1958) refers to singly reinforced members only. This method assumes that the extreme fibre of a beam farthest from the tensile steel shrinks in the same degree as the free shrinkage of the concrete, and the shrinkage curvature is calculated by formula:

$$\kappa_{cs} = \varepsilon_{cs} (1 - k_{cs}) / d; \quad k_{cs} = \varepsilon_{s,cs} / \varepsilon_{cs}, \tag{44}$$

where $\varepsilon_{s,cs}$ is the steel strain due to shrinkage. Miller suggested empirical values of coefficient k_{cs} equal to 0,1 for heavily reinforced members and 0,3 for moderately reinforced members.

8.5. Branson’s method

Branson’s method (1977: 169) represents a modification of Miller’s method. This method is applicable to both singly- and doubly-reinforced members. The shrinkage curvature of a member is derived by the formula:

$$\kappa_{cs} = \begin{cases} 0,7 \frac{\varepsilon_{cs}}{h} \sqrt[3]{\Delta p} \sqrt{\frac{\Delta p}{p}}, & \Delta p \leq 3,0 \%, \\ \varepsilon_{cs} / h, & \Delta p > 3,0 \%, \end{cases} \tag{45}$$

$$\Delta p = p - p'; \quad p = \frac{A_{s1}}{bd} \cdot 100\%; \quad p' = \frac{A_{s2}}{bd} \cdot 100\%.$$

This method is also suggested by British Standard Code and recommended by ACI 209 (ACI Committee 209 1998).

8.6. Corley & Sozen method

This method (Branson 1977: 171) is given by

$$\kappa_{cs} = \frac{0,035}{d} (\rho - \rho'); \quad \rho = \frac{A_{s1}}{bd}; \quad \rho' = \frac{A_{s2}}{bd}. \tag{46}$$

The constant 0,035 may be used for sections where the free shrinkage is known or where it is of the order of 500 micro-strains. In this case, the calculated curvature may be multiplied by the ratio of shrinkage to 500 micro-strains. This procedure is also recommended by *ACI* for the design of concrete bridges (Branson 1977: 171).

9. Analysis of shrinkage effect on deformational behaviour of RC beams

Two numerical analyses of shrinkage effect on deformational behaviour of RC beams are presented in this chapter. The test results reported by Фигаровский [Figarovskij] (1962) are used for this purpose. The experimental beams were cured under the laboratory conditions at average relative humidity (*RH*) 53 %. The beams of rectangular section, 3,0 m in span, were tested during 29 days under a four point bending system with 1,0 m pure bending zone. Basic parameters of the beams employed in the analyses are presented in Table 8.

Table 8. Parameters of test beams (Фигаровский [Figarovskij] 1962)

Beams	<i>h</i>	<i>d</i>	<i>b</i>	<i>a</i> ₂	<i>A</i> _{s1}	<i>A</i> _{s2}	<i>p</i>	<i>f</i> _{c,cube200}	<i>f</i> _y	<i>E</i> _s
	mm				mm ²		%	MPa		GPa
<i>P1-1Kk</i>	251	228	179	15	149,4	56,5	0,37	28,0	389	210
<i>P2-2Pk</i>	252	232	179	15	221,5	56,5	0,53	30,9	428	200
<i>P3-2Pd</i>	250	230	180	15	364,5	56,5	0,88	35,3	437	200

9.1. Prediction of shrinkage curvature

This sub-chapter presents a comparative analysis of predictions made by the methods discussed in Chapter 8. Shrinkage curvature of beam *P3-2Pd* (Table 8) was calculated. The calculation results are presented in Fig. 7. Fig. 7 also shows (by dashed vertical lines) shrinkage deformations calculated for the beam using the Eurocode 2 and the ACI 209 methods.

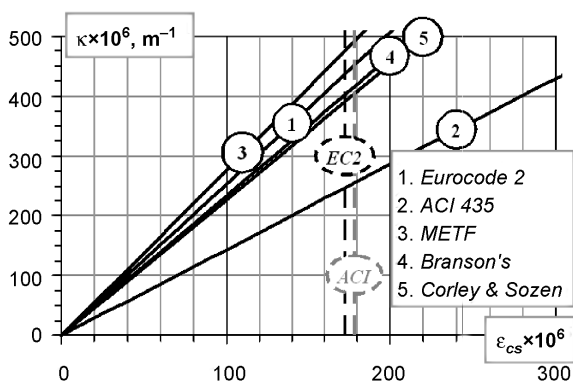


Fig. 7. Shrinkage curvatures of the beam *P3-2Pd* (Фигаровский [Figarovskij] 1962)

It can be noted that predictions made by most of the methods, ie *Eurocode 2*, Modified equivalent tensile force, Branson's and Corley & Sozen, are very close. The curvatures calculated (for a normative value of shrinkage strain) using these methods were 437, 493, 417 and $404 \times 10^{-6} \text{ m}^{-1}$, respectively. In contrast to this, the prediction by the *ACI 435* method was $256 \times 10^{-6} \text{ m}^{-1}$.

9.2. Numerical modelling the test beams

In this section, the deflection predictions made by *Eurocode 2* (CEN 2001) and *ACI 318* (ACI Committee

318 2005) code methods and the *layer model* (Kaklauskas 2004) are checked against the experiment data of RC beams reported by Фигаровский [Figarovskij] (1962). Deflections predicted by the codes are shown in Fig. 8.

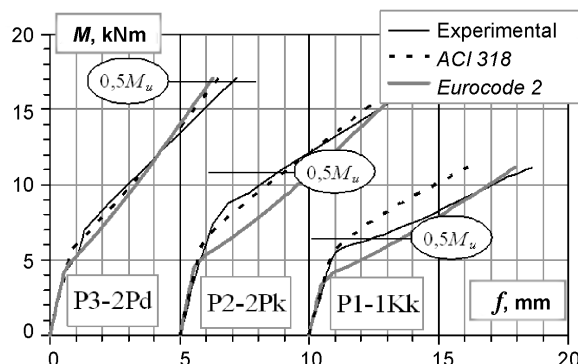


Fig. 8. Deflection of test beams (Фигаровский [Figarovskij] 1962) prediction by the code methods

In the *layer model* shrinkage was modelled by a fictitious axial force and bending moment as shown in Fig. 9 (see also Fig. 6). *Eurocode 2* technique was used for calculating free shrinkage strains. Concrete tensile and compressive strengths and modulus of elasticity were defined using *Eurocode 2*. An elastic-plastic relationship has been adopted for reinforcement material idealisation. The Eurocode 2 stress-strain relationship was assumed for the compressive concrete. A simple linear tension stiffening relationship shown in Fig. 10a was taken for modelling cracked tensile concrete. Factor β in this relationship was calculated using the relationship proposed by Kaklauskas (2001: 70):

$$\beta = 32,8 - 27,6 \cdot p + 7,12 \cdot p^2, \quad (47)$$

where *p* is the reinforcement ratio (%). Beam *P1-1Kk* was reinforced with plain bars, thus according recommendations (Kaklauskas 2001: 70), β was reduced by 20 %.

Experimental and calculated moment-deflection diagrams are shown in Fig. 10b. A good agreement of calculation results with experimental data, when shrinkage effect was taken into consideration, should be noted. Fig. 10b shows that shrinkage has significantly reduced the cracking resistance and leads to larger deflections. On average, deflections after cracking have increased about 15 % when shrinkage was taken into account. Table 9 presents a relative error of deflection predictions at service load (corresponding to 50 % of the ultimate bending moment *M_u*) including and ignoring shrinkage.

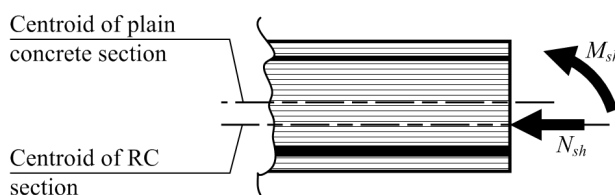


Fig. 9. Modelling the shrinkage in *layered model* by fictitious actions (axial force and bending moment)

Table 9. Relative error of deflection predictions at service loading

Beams	Relative error $(f_{calc} - f_{obs})/f_{obs}$, %			
	EC 2	ACI 318	Layer model	
			Shrinkage ignored	Shrinkage included
P1-1Kk	-49,8	37,4	54,8	41,8
P2-2Pk	-35,2	-6,24	35,4	12,3
P3-2Pd	12,4	9,3	16,7	4,1

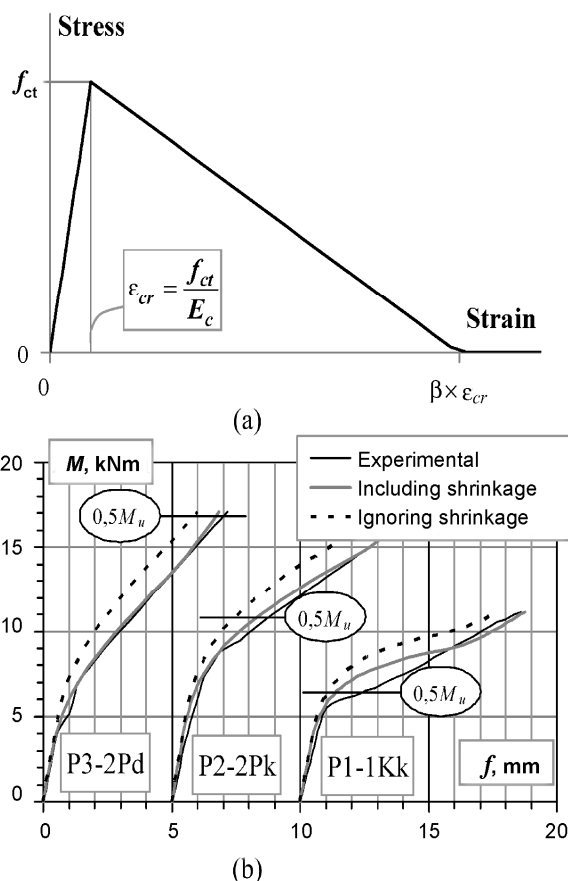


Fig. 10. Numerical modelling of test beams (Фигаровский [Figarovskij] 1962): stress-strain relationship used in the numerical analysis (a) and calculated moment-deflection relationships (b)

10. Concluding remarks

Beyond the uncertainties associated with the creep and the shrinkage characteristics in concrete, which are undoubtedly the biggest obstacle to improve the accuracy of deformation prediction, there are further uncertainties contributing to the deformation problem in RC structures. It seems evident that the shrinkage prediction models can be found in ϕ reasonable agreement when the parameters are in the range which is typical of an experimental setup in a laboratory. The availability of sufficient experimental data within that range provides a more solid basis for adjusting the theoretical models and the degree of uncertainty is smaller.

Shrinkage curvatures analysis has shown the difference in almost 1,7 times between predictions made by ACI 435 method and other methods.

Deflection analysis has shown that code methods indirectly take into account the shrinkage effect: the code predictions of cracking moment are in accordance with test results.

In the numerical short-term deflection analysis, shrinkage and creep effects have to be taken into account. The calculated deflections ignoring shrinkage were underestimated by about 15 %.

Acknowledgements

The authors wish to express their gratitude for the financial support provided by the Lithuanian State Fund of Research and Studies, and for the complementary financial support provided by the Agency of International Programs of Scientific and Technology Development in Lithuania.

References

ACI Committee 209. 1998. *Prediction of Creep, Shrinkage, and Temperature Effects in Concrete Structures*, ACI 209R-92 (Reapproved 1997). 47 p.

ACI Committee 318. 2005. *Building Code Requirements for Structural Concrete*, ACI 318-05. 430 p.

ACI Committee 435. 2003. *Control of Deflection in Concrete Structures*, ACI 435R-95 (Reapproved 2000). 89 p.

AL-Manaseer, A.; Lakshmikanth, S. 1999. Comparison between current and future design code models for shrinkage and creep, *Revue Française de Génie Civil* 3(3–4): 39–59.

AL-Manaseer, A.; Lam, J.-P. 2005. Statistical evaluation of shrinkage and creep models, *ACI Materials Journal* 102(3): 170–176.

Bangham, D. H.; Fackhoury, N. 1931. The swelling of charcoal, in *Proc of Royal Society of London* 130: 81–89.

Bazant, Z. P.; Baweja, S. 1995b. Justification and refinements of model b3 for concrete creep and shrinkage. Updating and Theoretical Basis, *Materials and Structures* 28(8): 488–495.

Bazant, Z. P.; Baweja, S. 1995a. Justification and refinements of model b3 for concrete creep and shrinkage. Statistics and sensitivity, *Materials and Structures* 28(7): 415–430.

Bazant, Z. P., et al. 1993. Preliminary guidelines and recommendation for characterizing creep and shrinkage in structural design codes, in *Proc of the 5th International RILEM Symposium Creep and Shrinkage of Concrete*, Barcelona, Spain, 1993, 805–829.

Bischoff, P. H. 2001. Effects of shrinkage on tension stiffening and cracking in reinforced concrete, *Canadian Journal of Civil Engineering* 28(3): 363–374.

Branson, D. E. 1977. *Deformation of Concrete Structures*. New York: McGraw-Hill, Inc. 546 p.

Comite Euro-International Du Beton. 1991. *CEB-FIB Model Code 1990: Design Code*. Thomas Telford. 437 p.

Comité Européen De Normalisation. 2001. *Eurocode 2: Design of Concrete Structures – Part 1: General Rules and Rules for Buildings*. Brussels: CEN. 230 p.

Federation Internationale Du Beton. 1999. *Structural Concrete. Textbook on Behaviour, Design and Performance*. Up-

- dated knowledge of the CEB/FIP Model Code 1990. 244 p.
- Gribniak, V.; Kaklauskas, G.; Bačinskas, D. 2007. State-of-art review on shrinkage effect on cracking and deformations of concrete bridge elements, *The Baltic Journal of Road and Bridge Engineering* 2(4): 183–193.
- Hua, C.; Ehrlicher, A.; Acker, P. 1995. Analyses and models of the autogenous shrinkage of hardening cement paste: i. modelling at macroscopic scale, *Cement and Concrete Research* 25(7): 1457–1468.
- Hua, C.; Ehrlicher, A.; Acker, P. 1997. Analyses and models of the autogenous shrinkage of hardening cement paste: ii. modeling at scale of hydrating grains, *Cement and Concrete Research* 27(2): 245–258.
- Ishida, T., et al. 1999. Microphysical approach to coupled autogenous and drying shrinkage of concrete, in *Proc. of International Workshop on Autogenous Shrinkage of Concrete, Hiroshima, Japan, 1998*. Taylor & Francis, 301–312.
- Kaklauskas, G. 2004. Flexural layered deformational model of reinforced concrete members, *Magazine of Concrete Research* 56(10): 575–584.
- Kaklauskas, G. 2001. *Integral Flexural Constitutive Model for Deformational Analysis of Concrete Structures*. 140 p.
- Koenders, E. A. B.; Van Breugel, K. 1997. Numerical modelling of autogenous shrinkage of hardening cement paste, *Cement and Concrete Research* 27(10): 1489–1499.
- Kovler, K.; Zhutovskiy, S. 2006. Overview and future trends of shrinkage research, *Materials and Structures* 39(9): 827–847.
- Meyerson, R., et al. 2002. *Evaluation of Models for Predicting (Total) Creep of Prestressed Concrete Mixtures*. Final Contract Report VTRC 03-CR5. Virginia: TRC. 55 p.
- Miller, A. 1958. Warping of reinforced concrete due to shrinkage, *ACI Journal Proceedings* 54(11): 939–950.
- Sakata, K.; Shimomura, T. 2004. Recent progress in research on and evaluation of concrete creep and shrinkage in Japan, *Journal of Advanced Concrete Technology* 2(2): 133–140.
- Sato, R., et al. 2007. Flexural behavior of reinforced recycled concrete beams, *Journal of Advanced Concrete Technology* 5(1): 43–61.
- Schellenberg, K., et al. 2005. Comparison of European and US practices concerning creep and shrinkage, in *Proc. of the fib Symposium Structural Concrete and Time, La Plata, 2005*, 445–452.
- Silliman, K. R.; Newton, C. 2006. Effect of misting rate on concrete shrinkage, in *Proc of HPC: Build Fast, Build to Last – 2006 Concrete Bridge Conference, Reno, Nevada, 2005*. PCA (CD). 19 p.
- Takács, P. F. 2002. *Deformations in Concrete Cantilever Bridges: Observations and Theoretical Modelling*. PhD dissertation. The Norwegian University of Science and Technology, Trondheim, Norway. 205 p.
- Weiss, W. J. 1999. *Prediction of Early-Age Shrinkage Cracking in Concrete*. PhD dissertation. Northwestern University, Evanston. 277 p.
- Zamblauskaitė, R.; Kaklauskas, G.; Bačinskas, D. 2005. Deformational analysis of prestressed high strength concrete members using flexural constitutive model, *Journal of Civil Engineering and Management* 11(2): 145–151.
- Фигаровский, В. В. 1962. Экспериментальное исследование жёсткости и трещиностойкости железобетонных изгибаемых элементов при кратковременном и длительном действии нагрузок: диссертация на соискание учёной степени кандидата технических наук [Figarovskij, V. V. Experimental research on rigidity and crack formation of reinforced concrete under short-time and durable loading]. Москва: НИИЖБ. 210 p.

BETONO TRAUKIMOSI ĮTAKA GELŽBETONINIŲ ELEMENTŲ ELGSENAI: SKAIČIAVIMO YPATUMAI

V. Gribniak, G. Kaklauskas ir D. Bačinskas

Santrauka

Straipsnyje atlikta betono traukimosi įtakos gelžbetoninių elementų elgsenai analizė, pateikta betono traukimosi deformacijų apskaičiavimo modelių apžvalga, aptarti traukimosi sukeltų kreivių nesimetriškai armuotuose gelžbetoniniuose elementuose apskaičiavimo metodai, taip pat pateikti nauji betono traukimosi eksperimentinių tyrimų duomenys. Aptarti veiksniai, turintys įtaką traukimosi deformacijoms, aprašytas supleišėjusių gelžbetoninių elementų trumpalaikių deformacijų apskaičiavimo algoritmas, rodantis traukimosi įtaką. Algoritmas pagrįstas *sluoksnių* modeliu ir vidutinių deformacijų koncepcija. Traukimosi įtaka gelžbetoninių sijų elgsenai nagrinėta, taikant normų bei *sluoksnių* metodus. Teoriniai rezultatai palyginti su literatūroje paskelbtais eksperimentinių tyrimų rezultatais. Parodyta, kad betono traukimas gerokai sumažina trumpalaikę apkrova veikiamų gelžbetoninių sijų atsparumą pleišėjimui bei lemia didesnes įlinkių reikšmes.

Reikšminiai žodžiai: traukimas, gelžbetonis, pleišėjimas, trumpalaikis apkrovimas, valkšnumas.

Viktor GRIBNIAK. Researcher at the Dept of Bridges and Special Structures, VGTU, Lithuania. BSc (2001, Civil Engineering) and MSc (2003, Building Structures) from VGTU. A study visit to Polytechnico di Torino (2003). Author of a number of papers. Research interests: mathematical modelling, statistical analysis and numerical simulation of concrete structures.

Gintaris KAKLAUSKAS. Professor and the Head of Dept of Bridges and Special Structures at VGTU, Lithuania. He received his engineering degree, PhD and Dr Habil (Dr Sc) from VGTU. Research interests include various topics of reinforced concrete, particularly constitutive modelling and numerical simulation of reinforced concrete structures. Recipient of Fulbright Fellowship (for research work at the University of Illinois, Urbana-Champaign, 1996) and Marie Curie Fellowship (experienced researcher category, 2002–2003). Member of the FIB Task Group 4.1 “Serviceability Models”.

Darius BAČINSKAS. Associate Professor of Dept of Bridges and Special Structures at Vilnius Gediminas Technical University (VGTU), Lithuania. He received his engineering degree, PhD (2002) from VGTU. Research interests: material constitutive models, non-linear numerical analysis of reinforced concrete structures.